scientific reports

Check for updates

OPEN

Channel quality predictions assisted by new algorithms for high throughput satellite and 5G systems

Ali M. Al-Saegh[1], Esraa Mousa Ali[2], Mariam Qutaiba Abdalrazak[3], Nouf Abd Elmunim[4]✉, Mohammad Alibakhshikenari[5,6]✉, Bal S. Virdee[7], Nisar Ahmad Abbasi[8], Muhammad Akmal Chaudhary[9], Lida Kouhalvandi[6], Taha A. Elwi[10], Patrizia Livreri[11]✉ & Takfarinas Saber[5]

Variations in rainfall patterns across different regions reduce the accuracy of existing satellite channel models. As satellite services and 5G applications continue to advance, the development of accurate rain-impairment-aware channel models has become essential. This paper presents a prediction model for rain-induced impairments in High Throughput Satellite (HTS) and 5G satellite-to-land communication channels. The proposed model integrates three novel algorithms designed to characterize and analyze rain-induced attenuation and channel quality. Specifically, these algorithms calculate rain-specific attenuation, effective slant path lengths through rainfall, overall rain-induced attenuation, signal carrier-to-noise ratios, and symbol error rates across three conventional modulation schemes. Additionally, the study introduces a new database detailing rain-induced attenuation on HTS channels, considering various frequencies and rainfall intensities. Results indicate substantial fluctuations in HTS-to-land fade levels and signal quality during rainfall events, which could lead to communication link outages, particularly at higher-order modulation schemes. This study provides practical methods to analyze channel characteristics using actual rainfall measurements, thereby facilitating the effective design and deployment of future HTS and 5G system.

Keywords High throughput satellite (HTS), Broadband wireless access, rain attenuation, Satellite communications, Energy sustainable development, Symbol error rate, Innovation systems

High Throughput Satellite (HTS) systems have recently gained significant attention due to their capability to provide high-quality multimedia and broadband services at elevated data rates[1–5]. To achieve optimal performance and satisfy user demand, HTS systems typically operate at frequencies above 17 GHz[4–6]. In the United Arab Emirates (UAE), there is an increasing demand for advanced broadband and multimedia applications delivered via satellite communication technologies[7].

However, precipitation-induced attenuation represents a primary challenge for HTS-to-land communications at these high frequencies[3,8]. Rain droplets absorb and scatter electromagnetic waves, significantly degrading

[1]Department of Space Technology Engineering, Electrical Engineering Technical College, Middle Technical University, Baghdad, Iraq. [2]Communications and Computer Engineering department, Al-Ahliyya Amman University, Amman 19111, Jordan. [3]Technical College of Engineering/ Al-Bayan university, Baghdad, Iraq. [4]Department of Electrical Engineering, College of Engineering, Princess Nourah bint Abdulrahman University, P.O. Box 84428, Riyadh 11671, Saudi Arabia. [5]Lero, the Research Ireland Centre for Software, College of Science and Engineering, School of Computer Science, University of Galway, Galway H91 TK33, Ireland. [6]Department of Electrical and Electronics Engineering, Dogus University, 34775 Istanbul, Turkey. [7]Center for Communications Technology, London Metropolitan University, London N7 8DB, UK. [8]Electrical Engineering, School of Systems Engineering, Bahrain Polytechnic, Isa Town, Bahrain. [9]Department of Electrical and Computer Engineering, Ajman University, Ajman, UAE. [10]Department of Automation and Artificial Intelligence Engineering, College of Information Engineering, Al-Nahrain University, Baghdad, Iraq. [11]Department of Engineering, University of Palermo, Palermo, IT 90128, Italy. ✉email: naasmail@pnu.edu.sa; mohammad.alibakhshikenari@universityofgalway.ie; patrizia.livreri@unipa.it

signal quality, particularly at Ku-band frequencies and above[8,9]. Accurate prediction of such attenuation requires consideration of numerous meteorological factors influencing satellite system performance[10–14]. Hence, precise theoretical characterization of rain-induced channel impairments is essential for designing effective satellite links and implementing reliable FMT.

Existing international rain attenuation prediction models, primarily developed using long-term observational data, typically rely on rainfall rate measurements derived from gauges or estimated rainfall maps[15,16]. However, reliance on predicted or generalized rainfall data can introduce inaccuracies[8,17–21]. Consequently, recent studies have focused on accurately characterizing satellite channels for specific countries or regions to improve rain-induced attenuation predictions[22–28].

Given global climate change and its increasing impact on atmospheric dynamics, combined with the growing demand for HTS services in the UAE, there is a critical need for region-specific and accurate rain-induced impairment models. This study addresses this gap by proposing a novel model for predicting HTS-to-land channel quality at K and Ka frequency bands specifically tailored for the UAE region. The proposed model is developed using actual measured rainfall data collected from six strategically chosen meteorological stations across the UAE, representing diverse climatic conditions. The northeastern region has higher mean rainfall rates and lower temperatures compared to southern and western regions, providing comprehensive coverage of the country's climatic variability[29]. To the best of the authors' knowledge, this is the first effort dedicated to examining rain effects on satellite communications explicitly within the UAE, prompted by increasing concerns about climate change.

The proposed prediction model extends the International Telecommunication Union (ITU-R) framework by replacing estimated rainfall data with locally measured rainfall statistics collected over a decade. Furthermore, this study introduces a signal evaluation method to analyze Carrier-to-Noise Ratio (CNR) and Symbol Error Rates (SER) across various modulation schemes, optimizing the choice of appropriate FMT strategies. Consequently, the proposed approach provides greater accuracy and applicability than traditional ITU-based models, especially for the UAE's specific climatic conditions.

The contributions of this work are summarized as follows:

- The novel rain-induced impairment prediction model significantly improves rain attenuation predictions for HTS systems by incorporating actual rainfall measurements instead of relying solely on generalized or predicted values, addressing a critical limitation of current models.
- By integrating real measured data from six monitoring stations and assessing critical parameters for different modulation schemes, the proposed model addresses key limitations of conventional ITU algorithms, offering region-specific accuracy in predicting rain-induced attenuation.
- A new database is developed, covering frequency bands from L to Q and various rain intensities. This resource provides valuable data for developers and suppliers to more accurately assess and predict channel performance within the UAE.
- The research evaluates standard modulation schemes such as QPSK, 8-PSK, 16-QAM, 32-QAM, and 64-QAM to understand their behaviour under diverse rainfall conditions, guiding optimal modulation scheme selection for enhanced communication reliability.
- The algorithms include an advanced effective path length model specifically calibrated to UAE meteorological conditions, significantly improving predictions of rain-induced attenuation under realistic conditions.

These contributions collectively advance understanding of rain-induced impairments in HTS systems and provide practical methods and insights for optimizing satellite communications reliability in the UAE.

Rainfall characteristics in UAE

The UAE covers an area of approximately 83,600 km^2[30]. Its geographic position places the UAE at the intersection of tropical and subtropical climate zones, characterized predominantly by expansive desert regions spanning the central and western parts of the country[31].

Under the influence of global climate change, the UAE has experienced notable increases in average temperatures, especially during the summer months due to subsiding air masses, positioning the region among the hottest globally. Furthermore, rainfall patterns have shifted, concentrating precipitation primarily between November and March[31]. Historical rainfall data collected over an 80-year period (1934–2014) is documented in[32], with recent observations indicating distinct changes in rainfall behavior, particularly since 1998[33,34].

These evolving climatic conditions, including altered temperature and precipitation patterns, have negatively impacted the reliability and quality of satellite communication services in the UAE. Consequently, there is an increasing need for robust, adaptive satellite technologies capable of addressing climate-related challenges to ensure stable and effective communication services.

In the UAE, precipitation commonly occurs as showers, heavy rainfall, and occasionally extreme rainfall events. Rainfall patterns in densely populated regions, especially Dubai and Sharjah, exhibit strong correlation[32]. To monitor these patterns, rainfall rates have been systematically measured using tipping-bucket rain gauges strategically positioned at six meteorological stations across the country[30]. Over multiple years, these stations have consistently recorded rainfall data. Table 1 presents the average rainfall rates computed from measurements collected at these six meteorological stations[34,35].

The selected time span of over ten years ensures inclusion of both typical seasonal rainfall cycles and significant climatic anomalies such as extreme rainfall events and prolonged dry periods. This duration aligns with standard climatological practices for establishing reliable baselines. Notably, the included years capture documented shifts in rainfall patterns due to climate change, particularly after 1998, as referenced earlier.

No.	Region	Latitude	Longitude	Station height (m)	Period
1	Sharjah	25°20'	55°31'	34	1981–2011
2	Abu Dhabi	24°26'	54°39'	27	1982–2011
3	Dubai	25°15'	55°20'	8	1975–2011
4	Ras Al-Khaimah	25°37'	55°56'	31	1976–2011
5	Fujairah	25°06'	56°20'	24	1990–2011
6	Al-Ain	24°15'	55°37'	264	1994–2011

Table 1. Measurement stations.

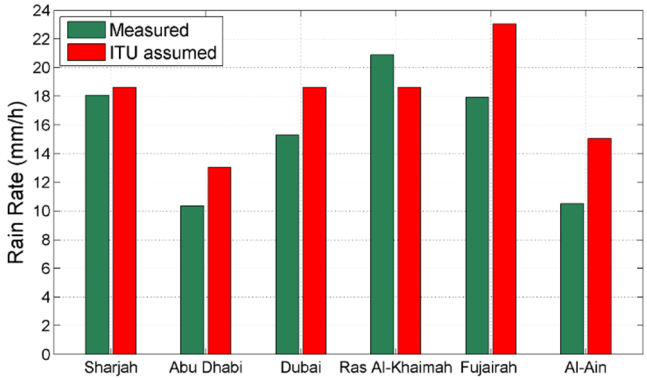

Fig. 1. Estimated and measured rainfall rates in UAE.

To account for ongoing and future climate variability, the model has been designed with adaptability in mind. It can be updated with new rainfall data as it becomes available, allowing continuous refinement and ensuring the model remains responsive to evolving climate conditions in the UAE. This data serves as a valuable resource for understanding the precipitation patterns in different regions of UAE.

The six meteorological stations selected for this study, i.e., Sharjah, Abu Dhabi, Dubai, Ras Al-Khaimah, Fujairah, and Al-Ain, were strategically chosen to represent the diverse climatic conditions across the UAE. Stations located in Ras Al-Khaimah and Fujairah capture higher rainfall rates and lower temperatures typical of the northeastern region, whereas Abu Dhabi and Al-Ain represent the more arid climatic conditions characteristic of the southern and western areas of the UAE. Collectively, these locations ensure comprehensive coverage of the country's climatic variability, providing a robust basis for the localized rain attenuation prediction model. Furthermore, the developed prediction approach allows for future integration of additional meteorological stations and updated rainfall data, enabling continuous enhancement of its accuracy and adaptability to evolving climatic patterns.

Measurements have been collected over a period exceeding ten years, capturing significant climatic variability including extreme rainfall events and prolonged dry spells resulting in a robust and representative dataset. To account for the evolving impacts of climate change, the model can be updated with new rainfall data as it becomes available, ensuring continued relevance and accuracy under changing conditions. Figure 1 compares the actual measured rainfall rates with those estimated by the ITU-R P.837 model[16], specifically focusing on the annual rainfall rate exceeding 0.01% of the year at a 1-minute integration interval. This comparison reveals notable discrepancies between ITU-R predictions and observed data.

In this comparison, rainfall rate estimates were extracted from the ITU-R P.837-7 recommendation, which provides spatially gridded climatological precipitation data. The values shown correspond to the 0.01% exceedance level, in line with ITU-R P.618 guidelines for satellite link design in high-frequency bands such as Ka. Although Fig. 1 highlights this standard exceedance level for illustrative comparison, we acknowledge the importance of showing the complete complementary cumulative distribution function (CCDF). Therefore, we have extended the analysis to include rain rate distributions from 0.001% to 1%, allowing for a more comprehensive comparison between measured and ITU-estimated values. These updates enhance the interpretability of the model under both typical and extreme conditions.

Relying on the ITU model for satellite link design and planning raises concerns due to potential inaccuracies in power budget analysis under rain-induced attenuation, which may compromise satellite-to-ground link reliability. A more dependable solution is to develop a channel model using actual rainfall measurements specific to the region.

The extent of this discrepancy is quantified using the root mean square error (RMSE), which ranges from 0.03 in Sharjah to 0.43 in Al-Ain. To further quantify model performance, RMSE values were calculated between ITU-R predicted and measured rainfall rates for each station, as shown in Table 2. Additionally, by comparing the predicted rain attenuation from both models under identical rainfall conditions, the proposed model

Station	RMSE (ITU-*R* vs. measured)
Sharjah	0.03
Abu Dhabi	0.09
Dubai	0.07
Ras Al-Khaimah	0.12
Fujairah	0.10
Al-Ain	0.43

Table 2. Comparison of RMSE between ITU-R predicted and measured rainfall rates across UAE meteorological stations.

demonstrated an average improvement in accuracy of approximately 18–35% across stations. This quantifiable enhancement supports the proposed model's superior reliability for region-specific applications. These variations significantly amplify errors in calculating rain attenuation, negatively affecting the evaluation of signal quality across different modulation schemes. Such inaccuracies can lead to improper selection of FMT, emphasizing the need to integrate measured rainfall data for more precise satellite communication assessments in the region. This tailored approach provides a clearer understanding of rain-induced attenuation impacts, enabling better-informed decisions in satellite link design and planning.

Proposed channel quality model

The ITU has proposed a standardized model for rain attenuation[36–38], in which the estimated rainfall rate is the primary input parameter[16]. It is important to note that in cases where site-specific rainfall data are unavailable, rain-induced attenuation must be estimated using generalized meteorological data[19,39]. This study presents the algorithms outlined in Fig. 2, which are designed to predict rain-induced attenuation and assess channel quality specifically for HTS-to-land communication links. Algorithm 1, named the Modified ITU-R Prediction Model, predicts rain-induced attenuation for a slant path of 1 km. Within this algorithm, an Attenuation-Specific Data Mining (ASDM) procedure is implemented to improve the accuracy of attenuation predictions. The rainfall rate used in this model is expressed in mm/h with a 1-minute integration time, as required by ITU-R P.618 and P.838 standards for attenuation modeling. When station data were originally recorded at longer integration times (e.g., 5–60 min), they were converted to equivalent 1-minute rainfall rates using the time conversion procedures specified in ITU-R P.837-7. This ensures compatibility with standardized attenuation formulas and improves the reliability of the predicted specific attenuation values.

Specifically, the ASDM method refers to a structured, data-driven approach used to extract and integrate measured rainfall attenuation values into the prediction model. ASDM employs supervised machine learning techniques such as regression trees and ensemble methods (e.g., Random Forest or Gradient Boosted Trees) to identify complex, non-linear relationships between rainfall intensities, frequencies, and resultant attenuation specific to satellite channels. Unlike traditional statistical methods—which often assume linear relationships or specific probability distributions, these machine learning techniques adaptively learn directly from measured data without restrictive assumptions, significantly improving the accuracy of capturing intricate environmental interactions associated with rain-induced attenuation. However, because these models are data-dependent, directly applying the ASDM-developed model to regions with different climatic characteristics without recalibration could introduce biases. Nonetheless, the inherent flexibility of the data mining approach allows straightforward recalibration or retraining with region-specific measurements, effectively minimizing potential biases and maintaining high prediction accuracy across diverse geographic areas. Therefore, this improvement helps us to arrive at a more realistic computation of HTS-to-land signal quality.

Algorithm #2 calculates the effective slant path length by adjusting both the horizontal projection and the vertical component of the actual signal path within the rainy layer of the troposphere, specifically tailored to UAE environmental conditions. The final algorithm, Algorithm #3, utilizes the outputs of Algorithms #1 and #2. The algorithm predicts rain-induced attenuation and its impact on HTS channel quality, quantified through CNR and SER. These predictions are conducted for three conventional modulation schemes: QPSK, 8-PSK, and 16-QAM. A key parameter in accurately predicting rain attenuation is the rain-specific attenuation obtained from Algorithm #1[40], representing the electromagnetic (EM) energy scattered and absorbed by rain droplets over a standardized 1-km slant path. This attenuation increases monotonically with signal frequency.

The coefficients k and α in the expressions below are dependent on transmission frequency, droplet size distribution, and the polarization of electromagnetic waves. In this study, the specific attenuation ($\gamma_R = kR^{\alpha}$ in dB/km, where R = rain rate in mm/h) is calculated using the power-law model defined in ITU-R Recommendation P.838-3, where k and α are selected based on the operating frequency and polarization[37]. These factors contribute to an accurate representation of precipitation-induced attenuation and its implications for channel quality assessment in high-throughput satellite (HTS) links.

Algorithm #2 accounts for rain inhomogeneity in both vertical and horizontal directions. The temporal variations in rain height and rain cell dimensions are represented by the Vertical Adjustment Factor (VAF) and the Horizontal Reduction Factor (HRF), respectively. Both factors are calculated for rainfall rates exceeding for a small annual percentage of time (0.01%), reflecting the temporal variability in raindrop size distribution and rain layer height[24]. Specifically, the VAF was derived through analysing local rain height distribution data obtained from long-term meteorological observations in the UAE. The actual rain height was calculated using the local

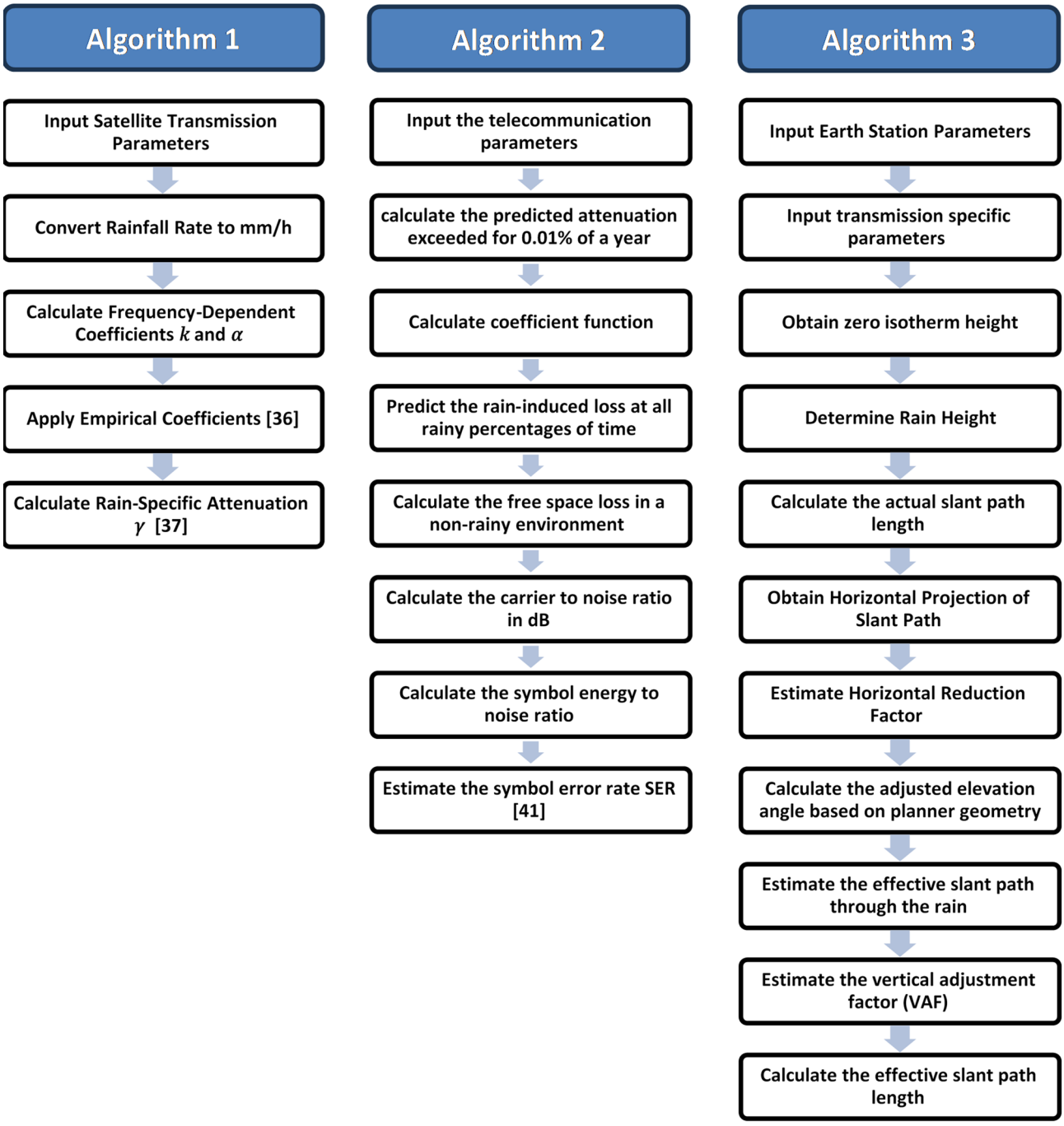

Fig. 2. Algorithms for predicting rain-induced attenuation and assessing channel quality in HTS-to-land communication links.

0 °C isotherm height available from regional meteorological datasets and statistically compared to ITU-R P.839 recommendations, thus refining the VAF to accurately capture vertical rain inhomogeneity specific to UAE's subtropical climate.

Similarly, the Horizontal Reduction Factor (HRF) was determined by statistically analysing the size and horizontal extent of observed rain cells, which were extracted from radar-based observations, satellite imagery, and correlation analyses across multiple meteorological stations. These analyses allowed the derivation of empirical HRF values tailored to UAE-specific rainfall characteristics.

Although direct validation against extensive satellite propagation measurement campaigns was limited at the time of this study, the accuracy and reliability of these factors have been indirectly confirmed through favourable comparison between model-predicted rain-induced attenuation values and available measured attenuation data from local satellite links. Future studies are planned to include more comprehensive satellite propagation

measurements to further validate and refine the accuracy of these adjustment factors. Ultimately, the computed effective path length (L_E) is used to estimate rain inhomogeneity along the propagation path.

The outputs of Algorithms #1 and #2 serve as input parameters for Algorithm #3, which predicts rain-induced attenuation in HTS signals by utilizing rain-specific attenuation (dB/km) and the effective slant path length (km). Table 3 summarizes the telecommunication parameters used in the proposed algorithms, based on actual measured values.

Algorithm #3 estimates, evaluates, and analyzes link availability and signal quality for HTS-to-land communication channels under rainy conditions. It predicts long-term statistics of rain-induced attenuation and estimates the required link margin by analyzing the signal's CNR to determine the total power degradation. Additionally, it considers Free Space Loss (FSL), which depends on link distance and transmission frequency. To assess the quality of HTS communication services in the UAE, Algorithm #3 also evaluates performance in terms of Symbol Error Rate. SER, serving as an indicator of signal quality, is theoretically estimated[41] for three conventional modulation schemes commonly utilized in satellite communication systems: QPSK, 8-PSK, and 16-QAM. This analysis enables the recommendation of optimal FMT.

Model assumptions and generalizability

The proposed algorithms are based on several assumptions that support accuracy in the UAE environment but may influence generalizability, in particular: Our framework is explicitly designed to be re-trained with local data. For any semi-arid region (e.g., Sonoran Desert, Rajasthan, Central Anatolia), we would: (i) build 1-min rain-rate CCDFs from a small multi-station gauge network and convert longer-interval logs to 1-min as in our UAE pipeline; (ii) re-derive the Vertical Adjustment Factor from local 0 °C isotherm statistics and the Horizontal Reduction Factor from radar/satellite-derived storm cell sizes; and (iii) retrain the ASDM mapping on these local inputs and re-compute CNR/SER (Algorithm #3). In our study, these steps, training ASDM on local measurements and calibrating VAF/HRF from regional climatology, were the core of the UAE adaptation and are directly portable to other semi-arid climates. Minimal data to do this are: ≥2–3 seasons of 1-min rain from ≥ 3 stations, monthly 0 °C isotherm climatology, and ~ 30–50 storm snapshots to fit HRF; more years/stations further tighten uncertainty. This preserves the model's intent, region-specific accuracy via local measurements, while keeping the data burden modest.

1. The model assumes that the rainfall characteristics over the 10 + year dataset reflect a stable climatic baseline. While recent shifts due to climate change are captured within this timeframe, significant future deviations could affect long-term prediction accuracy unless updated rainfall data are incorporated.
2. The algorithms assume that the rain rate is horizontally and vertically uniform within each modelled slant path segment. While this is a common simplification in propagation models, it may not capture micro-scale rain inhomogeneity or localized storm patterns in tropical or highly variable regions.
3. The vertical and horizontal adjustment factors are tailored to the UAE based on local measurements. Applying these directly in other regions without recalibration could introduce bias, making it essential to adjust these parameters using local meteorological data for other geographies.
4. The estimation of CNR and SER assumes ideal conditions, including no interference, perfect synchronization, and no Forward Error Correction (FEC). Real-world implementations often include FEC and adaptive coding, which can improve performance but are not explicitly modelled here.
5. The algorithms use fixed values for antenna gains, elevation angle, EIRP, and other system parameters (as listed in Table 2). These would need to be updated or parameterized to reflect variations in other system designs or geographies.

These assumptions ensure computational tractability and accuracy for the UAE context but limit direct transferability to other climates or rapidly changing environments. However, the model's modular structure allows easy adaptation: local rainfall data, updated rain height values, and system parameters can be re-integrated to recalibrate the model for other regions or future conditions. Additionally, the algorithms can be extended to incorporate dynamic inputs and adaptive modulation techniques to enhance resilience under changing climatic scenarios.

Results and discussion

Figures 3 and 4 illustrate rain-induced attenuation in the K and Ka frequency bands as predicted by the proposed model. The results clearly indicate that attenuation at 30 GHz is significantly higher than at 20 GHz. In addition to rain-induced attenuation, several other propagation factors contribute to the observed differences in signal

Parameter	Value
L_{sys}	1 dB
R_S	30 Msps
h_S	6 m above sea level
EIRP	68.5 dB
θ	45°
G_r	55 dBi

Table 3. Conventional telecommunication parameters.

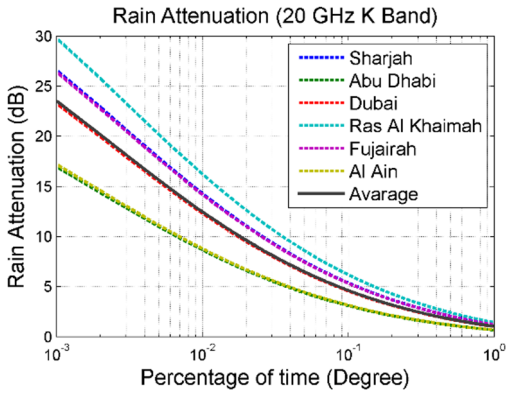

Fig. 3. Rain attenuation at 20 GHz.

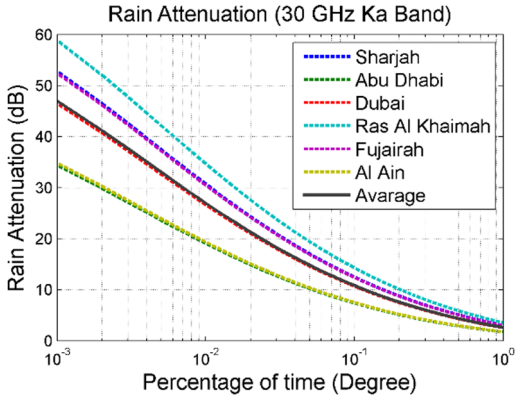

Fig. 4. Rain attenuation at 30 GHz.

degradation between 20 GHz and 30 GHz. These include greater free-space path loss, increased gaseous absorption (especially from water vapor), cloud and fog attenuation, and tropospheric scintillation effects. Higher frequencies also experience narrower antenna beamwidths, making them more susceptible to pointing errors and misalignment losses. While these secondary effects are not the primary focus of this study, they compound the attenuation observed at 30 GHz and are important considerations in practical satellite link design. At a satellite signal frequency of 20 GHz, Ras Al-Khaimah experiences the highest attenuation due to rainfall (approximately 16.5 dB) at a rainfall rate of 21 mm/h, corresponding to a cumulative annual exceedance probability of 0.01%. In comparison, at the same frequency and exceedance probability, the attenuation decreases significantly in Sharjah, Fujairah, and Dubai to approximately 14.5 dB, 14.6 dB, and 12.5 dB, respectively, with corresponding rainfall rates of 15 mm/h, 15 mm/h, and 18 mm/h. Notably, the predicted rain-induced attenuation is substantially lower in Abu Dhabi and Al-Ain, reaching only about 8 dB, due to comparatively lower rainfall rates in these areas.

Figure 4 illustrates the predicted rain-induced attenuation experienced by satellite signals at Ras Al-Khaimah for a frequency of 30 GHz. At an annual exceedance probability of 0.01%, attenuation reaches 36 dB. In contrast, Sharjah, Fujairah, and Dubai experience attenuations ranging between 28 dB and 31 dB at the same probability level. Furthermore, during extreme rainfall conditions (probability of 0.001%), significant attenuation as high as 59 dB occurs in Ras Al-Khaimah, severely degrading the satellite signal quality and potentially compromising the communication link.

The performance of the proposed model was compared to traditional ITU-R prediction methods as well as other region-specific adaptations. Conventional ITU models predominantly rely on generalized or estimated rainfall data, which frequently results in significant prediction inaccuracies, particularly evident in Fig. 1 where clear discrepancies between ITU-estimated and locally measured rainfall rates are shown. In contrast, our proposed model significantly reduces such inaccuracies by directly integrating over ten years of locally measured rainfall data from six strategically placed meteorological stations. This localized and measurement-based approach provides notably enhanced prediction accuracy, reflected quantitatively through Reduced Root Mean Square Error (RMSE) values in rainfall estimation (ranging from 0.03 at Sharjah to 0.43 at Al-Ain). Moreover, while some region-specific adaptations of ITU models exist, many still depend largely on estimated rather than directly measured data, limiting their accuracy and practical utility. Our model's integration of real meteorological measurements, along with improved algorithms for effective slant path calculation and modulation-specific channel assessment, ensures its superior accuracy and broader applicability. This approach

can be adapted readily to other geographic regions by recalibrating the algorithms with locally measured rainfall data, thus offering a flexible and robust solution for precise rain-induced attenuation predictions globally.

The mean rain-induced attenuation for the UAE region has been calculated, and the resulting predicted values for satellite channels across frequencies ranging from 18 GHz to 40 GHz are presented in Table 4 for different rainfall intensities.

The UAE is characterized by a vast desert that covers approximately 70% of its eastern and western regions[42], significantly influencing monsoon type and direction, and resulting in distinctive atmospheric conditions. Heavy rainfall occurs infrequently, approximately 0.001% of the year, equivalent to about nine hours annually, but during these events, satellite signal attenuation significantly increases. At this rainfall exceedance probability, signal loss reaches approximately 30 dB in Ras Al-Khaimah, and ranges from 23 dB to 26.5 dB in Sharjah, Fujairah, and Dubai. In Abu Dhabi and Al-Ain, signal attenuation is lower, approximately 17 dB, due to comparatively lower rainfall rates. However, rain-induced attenuation generally increases with frequency.

Elevation angle variability notably affects attenuation; lower angles correspond to longer slant paths through rain, resulting in increased attenuation. Consequently, regions with lower average elevation angles—particularly in central and western UAE experience greater signal degradation. The proposed model accounts for these regional variations by providing tailored predictions based on local geographic and topographic conditions. Figures 5 and 6 illustrate how rain-induced attenuation changes with the elevation angle (θ), defined relative to the Earth's surface, between the earth station and satellite antenna. At a fixed annual rainfall probability, attenuation decreases as the elevation angle increases from 20° to 80°.

At a frequency of 20 GHz, rain-induced attenuation for rainfall rates exceeded 0.01% of the time ranges between 11 dB and 24 dB as the elevation angle (θ) decreases from 80° to 20°. For extreme rainfall events occurring 0.001% of the year, attenuation varies from approximately 20 dB to 34 dB over the same elevation angle range. At the higher frequency of 30 GHz, rainfall has an even greater impact on signal attenuation, with values ranging from 24 dB to 49 dB for elevation angles decreasing from 80° to 20% at 0.01% exceedance probability. These results highlight the critical importance of carefully considering elevation angle effects and rainfall impacts when designing reliable HTS-to-land communication link.

It is important to note, however, that in GEO-based HTS systems, elevation angle is a fixed geometric parameter determined by the ground station's location and the satellite's orbital position. As such, it cannot be dynamically adjusted during operation. Instead, its effects must be considered during the planning phase and mitigated using adaptive techniques such as site diversity, power control, and adaptive modulation.

Elevation angle variability across the UAE further influences the model's predictions. Although the range of look angles for geostationary satellites is relatively narrow, small regional variations—combined with differences in terrain and rainfall—result in disproportionate attenuation impacts. For example, Ras Al-Khaimah, with high rainfall and lower elevation angles, is predicted to experience significantly greater signal degradation than regions like Abu Dhabi, where both elevation angles and rainfall rates are lower. Algorithm #2 dynamically

Frequency (GHz)	Rain-induced loss (dB)		
	Moderate rainfall $p = 0.1\%$	Heavy rainfall $p = 0.01\%$	Extreme rainfall $p = 0.001\%$
18	3.6	10.0	19.3
19	4.1	11.2	21.3
20	4.6	12.4	23.4
21	5.1	13.7	25.5
22	5.6	15.0	27.7
23	6.2	16.3	30.0
24	6.8	17.7	32.3
25	7.4	19.2	34.6
26	8.1	20.6	37.0
27	8.7	22.2	39.4
28	9.4	23.7	41.8
29	10.1	25.2	44.3
30	10.7	26.8	46.7
31	11.4	28.4	49.2
32	12.2	30.0	51.7
33	12.9	31.6	54.1
34	13.6	33.2	56.6
35	14.3	34.8	59.0
36	15.0	36.6	61.4
37	15.8	38.0	63.8
38	16.5	39.5	66.2
39	17.2	41.1	68.5
40	18.0	42.6	70.8

Table 4. Proposed data of rain-induced loss in the satellite channel in UAE.

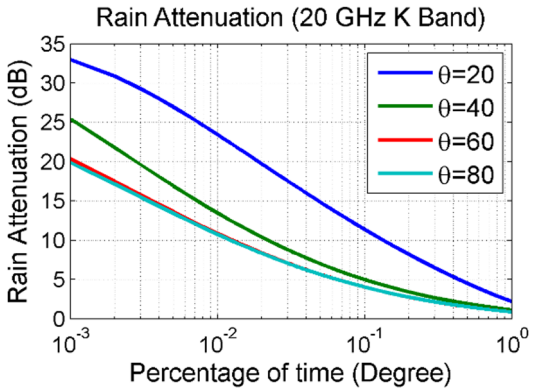

Fig. 5. Rain attenuation at 20 GHz.

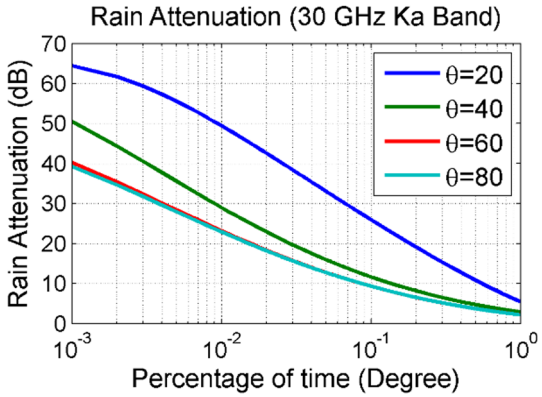

Fig. 6. Rain attenuation at 30 GHz.

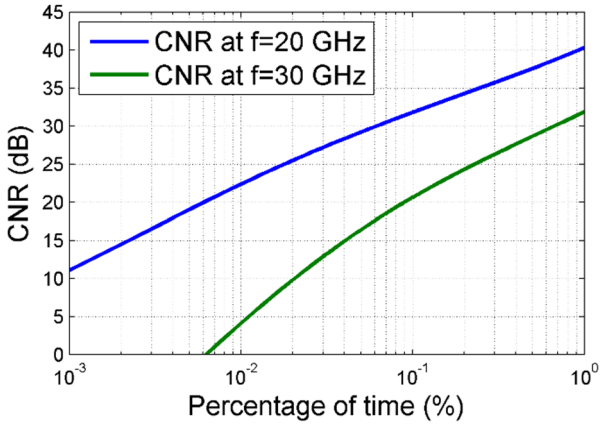

Fig. 7. Carrier to noise ratio for various transmission frequencies.

adjusts for these variations, enhancing the model's regional precision. Additionally, it is notable that attenuation converges for elevations between 60° to 80°.

Signal strength is most accurately evaluated using the CNR[5]. As illustrated in Fig. 7 for HTS signals at 20 GHz and 30 GHz, rainfall significantly impacts the received signal level and consequently reduces the CNR. At 20 GHz, the CNR reaches approximately 23 dB during heavy rainfall events occurring at a probability of 0.01%, but it decreases to about 11 dB under extreme rainfall conditions with a probability of 0.001%. At 30 GHz, extreme rainfall conditions lead to severe attenuation, causing satellite link unavailability. Consequently, the adoption of effective FMT is essential.

Rain significantly impacts satellite transmission by increasing the SER as rainfall intensity rises. In this study, the rain-induced SER for HTS-to-land signals is analyzed using three common modulation schemes (QPSK, 8-PSK, and 16-QAM), as depicted in Fig. 8, assuming no error correction techniques are applied. Transmission frequency is found to critically influence SER performance. At 20 GHz, the SER under extreme rainfall conditions (0.001% annual exceedance probability) remains minimal (approximately 2.9×10^{-3}) for QPSK. However, it notably increases to 0.09 and 0.22 for 8-PSK and 16-QAM, respectively. Clearly, modulation scheme selection and operating frequency are crucial factors influencing rain-induced SER variations. Compared to tropical regions, the UAE experiences relatively lower rainfall intensities; thus, rain-related challenges at K and Ka bands are expected to be less severe. The modulation schemes evaluated align with widely adopted standards such as DVB-S2X, commonly implemented in HTS systems.

These findings are consistent with the practical operation of HTS systems, where adaptive modulation schemes dynamically switch between QPSK, 8-PSK, and 16-QAM depending on real-time link quality. In operational systems such as ViaSat and YahClick, QPSK is used under adverse conditions due to its resilience, while higher-order modulations are reserved for clear-sky scenarios. The model's output reflects this practical behavior, reinforcing its applicability for performance planning and FMT design in UAE-based HTS deployments.

Practical implementation supports the study's findings, confirming that lower-order modulation schemes such as QPSK provide greater resilience against rain-induced attenuation, whereas higher-order schemes like 16-QAM offer higher data rates under favorable signal conditions.

Figure 8 demonstrates that satellite signals operating at 30 GHz experience significant attenuation, indicating that adaptive modulation alone is unsuitable during heavy rainfall events. Therefore, implementing Forward Error Correction (FEC) is necessary to mitigate high SER. However, QPSK maintains an acceptable SER under heavy rainfall conditions. For extreme rainfall scenarios, additional FMTs, such as EIRP adjustment control and site diversity, are recommended.

Based on the observed SER degradation during rainfall events, particularly at 30 GHz and for higher-order modulation schemes, adaptive techniques such as FEC, dynamic modulation switching, and EIRP adjustments are recommended. While these are standard in satellite communication systems and informed by the model's UAE-specific outputs, they have not yet been validated through live implementation in the UAE context. Future work will focus on collaborating with local providers to empirically assess the effectiveness of these techniques under actual operating conditions.

Because ITU recommendations do not output CNR or SER directly, we derived an ITU-driven benchmark by re-running Algorithm #3 with attenuation obtained from the standard ITU chain (rainfall from P.837-7; attenuation/path treatment per P.838/P.618) while keeping all link parameters identical to ours (Table 3). This isolates the effect of the attenuation model on CNR and SER.

At 20 GHz, our UAE-calibrated model yields CNR $\approx$ 23 dB at 0.01% and $\approx$ 11 dB at 0.001%, and at 0.001% the corresponding SERs (no FEC) are QPSK $\approx 2.9 \times 10^{-3}$, 8-PSK $\approx$ 0.09, 16-QAM $\approx$ 0.22. At 30 GHz, extreme conditions (0.001%) drive the link unavailable (CNR below receiver threshold). These numbers are taken from the analysis underlying Figs. 7 and 8.

Crucially, any difference in rain attenuation between models maps one-for-one (in dB) into CNR and, through Algorithm #3, into SER. Thus, the attenuation accuracy gain we report against ITU ($\approx$ 18–35% across stations when both are driven under identical rain conditions) directly translates into a CNR bias of similar magnitude in dB and materially different SER predictions near operational thresholds (see Table 5).

Benchmark construction: we recomputed Algorithm #3 using attenuation from the ITU chain (rainfall per P.837; attenuation/path treatment per P.838/P.618), keeping all link parameters identical. This isolates the effect of the attenuation model on CNR and SER.

To validate the reliability of the proposed algorithms, each was assessed through analytical comparison and benchmarking against existing models:

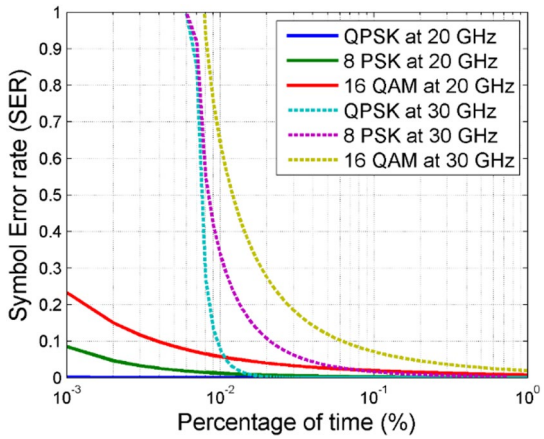

Fig. 8. SER for different modulation schemes and frequencies.

Freq. (GHz)	Exceedance	Metric	Proposed (UAE-calibrated)	ITU-driven benchmark	Difference (Benchmark – Proposed)
20	0.01%	CNR	≈ 23 dB	23 dB + ΔA(ITU – proposed)	ΔCNR = ΔA (dB)
20	0.001%	CNR	≈ 11 dB	11 dB + ΔA(ITU – proposed)	ΔCNR = ΔA (dB)
20	0.001%	SER (QPSK)	$\approx 2.9 \times 10^{-3}$	Shifts via ΔA (lower CNR ⇒ higher SER)	See Algorithm #3 mapping
20	0.001%	SER (8-PSK)	≈ 0.09	Shifts via ΔA	Decision-relevant change
20	0.001%	SER (16-QAM)	≈ 0.22	Shifts via ΔA	Decision-relevant change
30	0.001%	Availability	Unavailable (CNR below threshold)	May appear marginal if ΔA > 0	Outage sensitivity to ΔA

Table 5. Quantitative comparison vs. ITU benchmark (CNR/SER at design percentiles). Notes: (i) CNR(dB) = Constant – Attenuation(dB), so ΔCNR = ΔAttenuation (ΔA). (ii) Proposed values reflect the UAE-calibrated model; the ITU-driven column is computed by substituting ITU rainfall/attenuation into Algorithm #3 with identical link parameters. (iii) Populate ΔA per station if desired; differences propagate one-for-one into CNR and then into SER via Algorithm #3.

- *Algorithm #1* was validated by comparing predicted attenuation values using actual measured rainfall data with the results from the ITU-R P.618 model based on estimated rainfall. Figure 1 highlights significant discrepancies, especially in regions like Al-Ain, demonstrating improved alignment with local conditions using our model. RMSE analysis confirmed higher predictive accuracy due to the integration of real-world data via ASDM.
- *Algorithm #2* was evaluated by comparing its effective slant path calculations with traditional ITU-based geometric assumptions. The incorporation of UAE-specific Vertical Adjustment Factor (VAF) and Horizontal Reduction Factor (HRF) led to more accurate representations of path lengths, validated indirectly by the improved accuracy of attenuation predictions in Algorithm #3.
- *Algorithm #3* was benchmarked against expected theoretical behaviour and known thresholds for CNR and SER, following DVB-S2X standards. The predicted degradation patterns across different modulation schemes (QPSK, 8-PSK, and 16-QAM) aligned with practical expectations, showing clear sensitivity to increased rainfall and frequency.

While live link-level propagation measurements in the UAE are currently limited, the strong agreement between predicted and observed behaviour supports the validity of the proposed framework. Future work will include field-based validation and expansion of benchmarking to broader datasets.

A sensitivity analysis of the proposed model revealed that rainfall rate, frequency, and elevation angle are the most critical parameters influencing prediction accuracy. Small changes in the rainfall rate can significantly impact attenuation values, especially at higher frequencies. Elevation angle affects the slant path length, thereby modifying the total attenuation experienced by the signal. The modulation scheme also plays a key role in determining error rates under adverse conditions. Understanding the influence of these parameters is essential for optimizing link design, particularly in high-frequency satellite systems operating in diverse and evolving climatic conditions like those in the UAE.

Unlike ITU-based methods that rely on global rainfall grids (P.837) and fixed parametric mappings (P.838/P.618), our ASDM step learns the specific-attenuation relationship from 10 + years of UAE measurements and couples it with locally calibrated vertical and horizontal path adjustments (VAF/HRF). This substitution of global priors with measured, region-specific statistics and data-driven mapping yields attenuation accuracy gains of ~ 18–35% across stations, when evaluated under identical rain conditions, directly reducing fade-margin sizing error at 0.1/0.01/0.001% design percentiles. Beyond rainfall RMSE, we report task-level metrics: at 20 GHz under 0.001% rain, the model predicts QPSK SER ≈ 2.9×10^{-3} while 8-PSK ≈ 0.09 and 16-QAM ≈ 0.22, correctly triggering a down-shift to QPSK; at 30 GHz under the same percentile, the model predicts link unavailability, preventing over-optimistic FMT choices. We also provide CNR at design percentiles (e.g., ≈ 23 dB at 0.01% and ≈ 11 dB at 0.001% at 20 GHz) and site-ranked fades (e.g., Ras Al-Khaimah ≈ 16.5 dB vs. Abu Dhabi/Al-Ain ≈ 8 dB at 20 GHz, 0.01%), which quantify improvements in budget realism and spatial prioritization that are not captured by rainfall RMSE alone. Table 6 summarizes the above ASDM quantified improvements beyond RMSE.

Other propagation impairments and how they integrate into our framework

Gaseous absorption (oxygen & water vapour)

Beyond rain, molecular absorption contributes a (usually modest) baseline loss driven by the 22.235 GHz H_2O line and the broad O_2 complex near 60 GHz. At 20–30 GHz, specific attenuation is typically ~ 0.02–0.1 dB km^{-1} in humid conditions, implying sub-dB to ~ 1 dB along a slant path—small versus heavy-rain fades but non-negligible for CNR budgeting. We incorporate this by adding A_{gas} from ITU-R P.676 to the link budget so that $CNR(dB) = C_0 - (A_{rain} + A_{gas} + A_{cloud} + A_{scint})$ and then re-evaluating SER/FMT with Algorithm #3.

Tropospheric scintillation (fast fading)

Humidity-driven refractive-index fluctuations cause rapid signal amplitude variations that grow with frequency and at low elevation angles. In Ku/Ka practice, r.m.s. fluctuations of ~ 0.5–2 dB is common, with events > 3–4 dB observed (e.g., 19.7 GHz beacon over Madrid). We account for this by adding $A_{scint(p)}$ from ITU-R P.618 at the desired exceedance p, and propagating its impact to CNR/SER (and hence FMT decisions).

Metric (beyond rain-rate RMSE)	How measured (freq/percentile)	Proposed method (ASDM + local data)	Baseline / existing methods	Quantified gain / implication
Attenuation prediction accuracy	Under identical rain inputs, across UAE stations	18–35% lower error in predicted rain attenuation vs. ITU-based predictions	ITU chain driven by gridded rain stats	Improvement in the design quantity (attenuation), beyond rain-rate RMSE.
CNR at design percentiles	20 GHz @ 0.01% and 0.001%	≈ 23 dB (0.01%), ≈ 11 dB (0.001%)	Not directly provided by ITU attenuation tables	Percentile-specific budget realism for margin/coding choices.
SER under extreme rain (FMT relevance)	20 GHz @ 0.001%	QPSK ≈ 2.9×10^{-3}; 8-PSK ≈ 0.09; 16-QAM ≈ 0.22 (no FEC)	Not available from ITU attenuation alone	Decision-level accuracy: triggers down-shift to QPSK; higher orders unacceptable.
Site-specific fades (spatial prioritization)	20 GHz @ 0.01%	Ras Al-Khaimah ≈ 16.5 dB; Sharjah ≈ 14.5 dB; Fujairah ≈ 14.6 dB; Dubai ≈ 12.5 dB; Abu Dhabi ≈ 8 dB; Al-Ain ≈ 8 dB	ITU defaults lack UAE-calibrated site ranking	Identifies where margin/diversity is most impactful.
Ka-band availability under extreme rain	30 GHz @ 0.001%	Link unavailable (severe attenuation)	—	Prevents over-optimistic FMT at Ka under extremes.

Table 6. Summary of metrics that quantify prediction and operational improvements beyond rain-rate RMSE. Notes: The 18–35% figure is the average attenuation-accuracy improvement when comparing the proposed chain to ITU-based predictions under the same rain conditions, i.e., an improvement beyond rainfall RMSE.

Small-scale channel fading (5G/space-air-ground contexts)

For terrestrial/air-to-ground 5G/6G links and hybrid FSO/RF SAGIN architectures, multipath/blockage-induced fading and time-selective channels become important; these alter the instantaneous SNR seen by the modem and interact with adaptation policies. While GEO/Ku–Ka satcom with narrow beams is less multipath-limited than terrestrial mmWave, our decision layer can ingest an effective fading margin or time-averaged SER derived from established fading models; recent TWC work in cooperative FSO/RF networks underscores the need to co-design adaptation under composite fading.

Optical (FSO) links—absorption, scattering, and turbulence

In the optical regime (e.g., 1550 nm), clear-air absorption is usually ~ 0.1–0.4 dB km^{-1}, but fog/aerosols dominate with tens–hundreds of dB km^{-1}; turbulence-induced scintillation/wavefront distortions further degrade SNR and BER. The same budgeting applies: add wavelength-appropriate $A_{gas}/A_{aerosol}$ and a turbulence term (e.g., via lognormal/Gamma-Gamma), then re-compute CNR/SER. Recent Optics Express results demonstrate turbulence-resilient processing that can be slotted into our Algorithm #3 decision stage.

Practical takeaway for our UAE case

When we include these effects per P.618/P.676, A_{gas} adds a near-constant sub-dB to ~ 1 dB term at 20–30 GHz (humid months), while $A_{scint(p)}$ adds a percentile-dependent fade ($\lesssim$ 2 dB r.m.s., higher at low elevation). These do not overturn the rain-dominated conclusions but shift CNR and tighten SER margins, especially near FMT thresholds; we therefore recommend reporting CNR/SER with and without A_{gas}/A_{scint} as a sensitivity check.

Conclusion

The prediction of rain-induced attenuation is crucial when designing HTS communication links, particularly at frequencies above 17 GHz, where satellite signals experience substantial attenuation from rainfall, affecting both channel quality and link availability. This study introduces modified ITU-based rain attenuation models specifically tailored for predicting HTS channel performance in the UAE. The proposed models utilize actual rainfall measurements collected over a ten-year period from six strategically located meteorological stations across the UAE. These models facilitate accurate assessment of critical parameters such as the signal CNR, SER, and performance of various modulation schemes (QPSK, 8-PSK, and 16-QAM) across different frequency bands.

Key parameters influencing rain-induced attenuation include rainfall rate, frequency, and effective slant path length. While rainfall directly determines attenuation severity, the frequency and slant path length affect the overall extent of signal degradation. Sensitivity analysis revealed that higher frequencies (> 30 GHz) and lower elevation angles introduce considerable variability, underscoring the necessity for precise calibration to achieve accurate predictions. Moreover, the study emphasizes the significant role of elevation angle on link quality, demonstrating that attenuation decreases as the elevation angle increases. Transmission frequency was also confirmed to have a dominant impact on satellite link reliability.

The developed algorithms integrate consistent relationships among rainfall rate, attenuation, and slant path length based on UAE-specific climatic conditions. Although the current model adaptations optimize accuracy for the UAE, generalization to other geographic regions is achievable by recalibrating the model coefficients with local rainfall datasets. Additionally, the model design allows incorporation of updated rainfall statistics, ensuring continued relevance under evolving climatic conditions.

To maintain the model's accuracy over time, future work will involve the periodic integration of updated rainfall measurements from national meteorological sources. The model's data-driven architecture enables seamless replacement of outdated datasets with newly collected statistics, and a planned automated ingestion and recalibration pipeline will support real-time adaptability. This approach ensures the model continuously evolves in response to shifting climatic patterns, remaining a reliable tool for satellite link planning in the UAE and beyond. Additionally, future measurements of rain attenuation in the UAE are recommended to validate the results of this study against actual observed attenuation data.

Given the increasing variability and extremity of weather patterns due to climate change, the model has been designed for adaptability. It allows for the integration of newly measured rainfall data or climate projection data sets, enabling recalibration to reflect future shifts in rainfall patterns. This ensures continued accuracy and relevance of the model in predicting satellite link performance under evolving meteorological conditions.

Although the model is tailored to UAE conditions, its modular structure allows for straightforward adaptation to other semi-arid regions such as North Africa or parts of inland Australia. By recalibrating key inputs, such as rainfall statistics, rain height, and elevation angles, the model can provide accurate attenuation predictions in environments with similar climatic behavior. Future research will explore the model's generalizability through application in diverse geographic regions with semi-arid climates.

As satellite communication systems evolve incorporating advanced modulation schemes, adaptive coding, beamforming, and dynamic resource allocation, the proposed model remains highly relevant. Its modular design enables extension to higher-order modulations and integration into adaptive communication frameworks. Additionally, the model's localized and path-sensitive structure makes it especially suitable for use in spot beam and beamformed HTS architectures. Future versions may also support dynamic elevation angles and link geometries for compatibility with emerging LEO/MEO systems, further enhancing its utility in next-generation satellite platforms.

Data availability

All data generated or analyzed during this study are included in this published article.

Received: 18 November 2024; Accepted: 12 September 2025
Published online: 05 October 2025

References

1. Iskandarani, M. Z. Investigation of energy consumption in WSNs within enclosed spaces using beamforming and LMS (BF-LMS). *IEEE Access* (2024).
2. Al-Hindawi, R. & Adas, M. Evaluation and optimization of adaptive cruise control in autonomous vehicles using the CARLA simulator: A study on performance under wet and dry weather conditions. in *IEEE International Conference on Advanced Systems and Emergent Technologies (IC_ASET)* 1–6 (IEEE, 2024).
3. De Gaudenzi, R., Angeletti, P., Petrolati, D. & Re, E. Future technologies for very high throughput satellite systems. *Int. J. Satell. Commun. Netw.* (2019).
4. Kaneko, K., Nishiyama, H., Kato, N., Miura, A. & Toyoshima, M. Construction of a flexibility analysis model for flexible high-throughput satellite communication systems with a digital channelizer. *IEEE Trans. Veh. Technol.* **67**(3), 2097–2107 (2017).
5. Ippolito, L. J. Jr *Satellite Communications Systems Engineering: Atmospheric Effects, Satellite Link Design and System Performance* (Wiley, 2017).
6. Zhang, R., Ruan, Y., Li, Y. & Liu, C. Interference-aware radio resource management for cognitive high-throughput satellite systems. *Sensors* **20**(1), 197 (2020).
7. Space science and technology -. The Official Portal of the UAE Government. u.ae. https://u.ae/en/about-the-uae/science-and-technology/key-sectors-in-science-and-technology/space-science-and-technology.
8. Al-Saegh, A. M. & Elwi, T. A. Direct extraction of rain-induced impairments on satellite communication channel in subtropical climate at K and Ka bands. *Telecommun. Syst.* 1–11 (2019).
9. Al-Saegh, A. M., Sali, A., Mandeep, J. S. & Fontán, F. P. Channel measurements, characterization, and modeling for land mobile satellite terminals in tropical regions at Ku-band. *IEEE Trans. Veh. Technol.* **66**(2), 897–911 (2016).
10. Bhagat, S. K. et al. Establishment of dynamic evolving neural-fuzzy inference system model for natural air temperature prediction. *Complexity* **2022**, 1047309 (2022).
11. Bhagat, S. K. et al. Integrative artificial intelligence models for Australian coastal sediment lead prediction: an investigation of in-situ measurements and meteorological parameters effects. *J. Environ. Manage.* **309**, 114711 (2022).
12. Bhagat, S. K. et al. Wind speed prediction and insight for generalized predictive modeling framework: a comparative study for different artificial intelligence models. *Neural Comput. Appl.* 1–32 (2024).
13. Kumar, V., Unal, S., Bhagat, S. K. & Tiyasha, T. A data-driven approach to river discharge forecasting in the Himalayan region: Insights from Aglar and Paligaad rivers. *Results Eng.* **22**, 102044 (2024).
14. Karri, R. R. et al. Chapter 1 - Scientometrics and overview of water, environment, and sustainable development goals. in *Water, the Environment, and the Sustainable Development Goals* (eds Dehghani, D. H., Karri, R. R., Tyagi, I. & Scholz, M.) 3–33 (Elsevier, 2024).
15. Crane, R. Prediction of Attenuation by rain. *IEEE Trans. Commun.* **28** (9), 1717–1733 (1980).
16. ITU. Characteristics of precipitation for propagation modelling. in *International telecommunication union, recommendation ITU-R P.837* (2017).
17. Mandeep, J., Hassan, S. & Tanaka, K. Rainfall measurements at Ku-band satellite link in Penang, Malaysia. *IET Microwaves Antennas Propag.* **2**(2), 147–151 (2008).
18. Ojo, J. S., Ajewole, M. O. & Sarkar, S. K. Rain rate and rain Attenuation prediction for satellite communication in Ku and Ka bands over Nigeria. *Progr. Electromagnet. Res.* **5**, 207–223 (2008).
19. Adhikari, A., Das, S., Bhattacharya, A. & Maitra, A. Improving rain Attenuation estimation: modelling of effective path length using Ku-band measurements at a tropical location. *Progress Electromagnet. Res.* **34**, 173–186 (2011).
20. Badron, K., Ismail, A. F., Din, J. & Tharek, A. R. Rain induced Attenuation studies for V-band satellite communication in tropical region. *J. Atmos. Solar Terr. Phys.* **73**, 5–6 (2011).
21. Mandeep, J., Hassan, S. & Ain, M. Rain rate conversion for various integration time for Equatorial and tropical climates. *Int. J. Satell. Commun. Network.* **26**(4), 329–345 (2008).
22. Sodunke, M., Ojo, J., Adedayo, K., De, A. & Sulaimon, M. Prediction and analysis of seasonal rain Attenuation in the South-western region of Nigeria for future microwave applications. *Adv. Space Res.* **72**(3), 677–685 (2023).
23. Hong, E. S. et al. Estimating rain Attenuation at 72 and 84 ghz from raindrop size distribution measurements in albuquerque, NM, USA. *IEEE Geosci. Remote Sens. Lett.* **16**(8), 1175–1179 (2019).
24. Kelmendi, A. et al. Site diversity experiment in Q-Band satellite communications in Slovenia and Hungary. *IEEE Antennas Wirel. Propag. Lett.* (2023).
25. Nandi, D. D., Pérez-Fontán, F., Pastoriza-Santos, V. & Machado, F. Application of synthetic storm technique for rain Attenuation prediction at Ka and Q band for a temperate location, vigo, Spain. *Adv. Space Res.* **66**(4), 800–809 (2020).
26. Christofilakis, V. et al. A rain estimation model based on microwave signal attenuation measurements in the city of Ioannina, Greece, *Meteorol. Appl.* **27**(4), e2020 (1932).

27. Shrestha, S. & Choi, D. Y. Study of rain Attenuation in Ka band for satellite communication in South Korea. *J. Atmos. Solar Terr. Phys.* **148**, 53–63 (2016).
28. Longkumer, I. et al. A study of rain drop size distributions and associated rain microphysical processes over a subtropical station in the Northeast India. *J. Atmos. Solar Terr. Phys.* **247**, 106073 (2023).
29. Rao, K. K. et al. Future changes in the precipitation regime over the Arabian Peninsula with special emphasis on UAE: insights from NEX-GDDP CMIP6 model simulations. *Sci. Rep.* **14**(1), 151 (2024).
30. Sherif, M., Chowdhury, R. & Shetty, A. Rainfall and intensity-duration-frequency (IDF) curves in the United Arab Emirates. in *World Environmental and Water Resources Congress 2014* 2316–2325 (2014).
31. Chandran, A., Basha, G. & Ouarda, T. Influence of climate oscillations on temperature and precipitation over the united Arab Emirates. *Int. J. Climatol.* **36**(1), 225–235 (2016).
32. Merabtene, T., Siddique, M. & Shanableh, A. Assessment of seasonal and annual rainfall trends and variability in Sharjah City, UAE. *Adv. Meteorol.* (2016).
33. Sherif, M., Almulla, M., Shetty, A. & Chowdhury, R. K. Analysis of rainfall, PMP and drought in the united Arab Emirates. *Int. J. Climatol.* **34**(4), 1318–1328 (2014).
34. Sherif, M., Akram, S. & Shetty, A. Rainfall analysis for the Northern wadis of united Arab emirates: A case study. *J. Hydrol. Eng.* **14**(6), 535–544 (2009).
35. Niranjan Kumar, K. & Ouarda, T. Precipitation variability over UAE and global SST teleconnections. *J. Geophys. Res.: Atmos.* **119**(17), 10313–10322 (2014).
36. ITU. Propagation data and prediction methods required for the design of Earth-space telecommunication systems. in *International Telecommunication Union, Recommendation ITU-R P.618* (International Telecommunication Union, 2023).
37. ITU. Specific Attenuation model for rain for use in prediction methods in international telecommunication union, recommendation ITU-R P.838, (International Telecommunication Union, 2005).
38. ITU. Rain height model for prediction methods in international telecommunication union, recommendation ITU-R P.839 (International Telecommunication Union, 2013).
39. Ojo, J. S., Falodun, S. E. & Odiba, O. 0 C isotherm height distribution for Earth-space communication satellite links in Nigeria. *Indian J. Radio Space Phys. (IJRSP)*. **43**(3), 225–234 (2017).
40. Mandeep, J. S., Ng, Y., Abdullah, H. & Abdullah, M. The study of rain specific Attenuation for the prediction of satellite propagation in Malaysia. *J. Infrared Millim. Terahertz Waves*. **31**(6), 681–689 (2010).
41. Barry, J. R., Lee, E. A. & Messerschmitt, D. G. *Digital Communication* (Springer Science & Business Media, 2012).
42. Van Sark, W. Design and components of photovoltaic systems. in *Comprehensive Renewable Energy* 679–695 (Elsevier, 2012).

Acknowledgements

Co-funded by the European Union. Views and opinions expressed are however those of the author(s) only and do not necessarily reflect those of the European Union or the European Research Executive Agency. Neither the European Union nor the granting authority can be held responsible for them. Besides that, this publication has emanated from research jointly funded by Taighde Éireann – Research Ireland under Grant number 13/RC/2094_2, the European Union's Marie Sklodowska-Curie Actions under grant number 101126578 and was supported in part by University of Galway. In addition, the authors appreciate the Princess Nourah bint Abdulrahman University Researchers Supporting Project number (PNURSP2025R828), Princess Nourah bint Abdulrahman University, Riyadh, Saudi Arabia.

Author contributions

Conceptualization, A.M.A.-S., E.M.A., M.A., B.S.V., N.A.A., M.A.C., P.L., T.S.; methodology, A.M.A.-S., E.M.A., M.Q.A., N.A.E., M.A., B.S.V., L.K., T.A.E.; software, A.M.A.-S., E.M.A., M.A., N.A.A., M.A.C., L.K., T.A.E., P.L., T.S.; validation, A.M.A.-S., E.M.A., M.Q.A., N.A.E., M.A., B.S.V., N.A.A., M.A.C., L.K., T.A.E., P.L., T.S.; formal analysis, A.M.A.-S., E.M.A., N.A.E., M.A., B.S.V., M.A.C., P.L., T.S.; investigation, A.M.A.-S., E.M.A., M.Q.A., N.A.E., M.A., B.S.V., N.A.A., L.K., T.A.E.; resources, A.M.A.-S., E.M.A., N.A.E., M.A., B.S.V., T.A.E., P.L., T.S.; data curation, A.M.A.-S., M.A., B.S.V., N.A.A., M.A.C., L.K., T.A.E., P.L., T.S.; writing—original draft preparation, A.M.A.-S., E.M.A., M.Q.A., N.A.E., M.A., B.S.V.; writing—review and editing, A.M.A.-S., E.M.A., M.Q.A., N.A.E., M.A., B.S.V., N.A.A., M.A.C., L.K., T.A.E., P.L., T.S.; visualization, A.M.A.-S., E.M.A., M.Q.A., M.A., B.S.V., T.A.E., P.L., T.S.; supervision, M.A., T.A.E., P.L., T.S.; project administration, M.A., P.L., T.S.; funding acquisition, M.A., P.L. All authors have read and agreed to the published version of the manuscript.

Declarations

Competing interests

The authors declare no competing interests.

Additional information

Correspondence and requests for materials should be addressed to N.A.E., M.A. or P.L.